Proceeding Paper

Probing Light Mediators and Neutrino Electromagnetic Moments with Atomic Radiative Emission of Neutrino Pairs [†]

Shao-Feng Ge [1,2,*,‡] (ID) **and Pedro Pasquini** [1,2,3,*,‡] (ID)

1   Tsung-Dao Lee Institute & School of Physics and Astronomy, Shanghai Jiao Tong University, Shanghai 200240, China
2   Key Laboratory for Particle Astrophysics and Cosmology (MOE) & Shanghai Key Laboratory for Particle Physics and Cosmology, Shanghai Jiao Tong University, Shanghai 200240, China
3   Department of Physics, University of Tokyo, Bunkyo-ku, Tokyo 113-0033, Japan
*   Correspondence: gesf@sjtu.edu.cn (S.-F.G.); pedrosimpas@g.ecc.u-tokyo.ac.jp (P.P.)
†   Presented at the 23rd International Workshop on Neutrinos from Accelerators, Salt Lake City, UT, USA, 30–31 July 2022.
‡   These authors contributed equally to this work.

Abstract: We present the novel idea of using the atomic radiative emission of neutrino pairs to test physics beyond the Standard Model, including light vector/scalar mediators and the anomalous neutrino electromagnetic moments. With $\mathcal{O}(\text{eV})$ momentum transfer, atomic transitions are particularly sensitive to light mediators and can improve their coupling strength sensitivity by 3~4 orders of magnitude. In particular, the massless photon belongs to this category. The projected sensitivity with respect to neutrino electromagnetic moments is competitive with dark matter experiments. Most importantly, neutrino pair emission provides the possibility of separating the electric and magnetic moments, even identifying their individual elements, which is not possible by existing observations.

Keywords: neutrino; beyond standard model; light mediators; neutrino magnetic moments

1. Introduction

The neutrino oscillation, and hence neutrinos being massive, have been experimentally established as the first new physics beyond the Standard Model (BSM) of particle physics. However, the reason behind massive neutrinos, and in particular non-standard interactions (NSIs), retain various possibilities [1–4]. This is especially true for light mediators. A mediator with mass m and coupling g produces a matrix element $|\mathcal{M}|^2 \sim g^4/(q^2 + m^2)^2$. For $m^2 \ll q^2$, the contribution of a light mediator is typically suppressed by the momentum transfer, $|\mathcal{M}|^2 \sim g^4/q^4$. To improve the sensitivity, smaller momentum transfer $q^2 \lesssim m^2$ is better.

Laboratory-based experiments typically have momentum transfer at the keV~MeV scale, which makes it difficult to constrain very light mediators. In this work, we present a new possibility: we propose using the atomic radiative emission of neutrino pairs (RENP) [5–8] to look for light mediators. With intrinsically $\mathcal{O}(\text{eV})$ energy, RENP provides a suitable environment to significantly improve the sensitivity of searching light particles.

Our study proceeds in two steps: (1) a general light vector/scalar mediator between electron and neutrino [9] and (2) the neutrino electric and magnetic moment interactions with a massless photon [10]. The latter is particularly interesting. Energy thresholds can be used to separate the electric from the magnetic moments and probe their individual elements. With a suitable design, future RENP experiments can greatly improve the sensitivity on BSM mediators and NSI.

2. Atomic Radiative Emission of Neutrino Pairs

The RENP is an atomic E1×M1 transition from an atomic excited state $|e\rangle$ to a ground state $|g\rangle$ via an intermediate virtual state $|v\rangle$ with energies $E_v > E_e > E_g$ [5–8,11,12]. A neutrino pair is emitted in the transition $|e\rangle \to |v\rangle$ and a photon is emitted in $|v\rangle \to |g\rangle$.

The whole reaction chain is

$$|e\rangle \to \nu\bar{\nu} + |v\rangle(\to |g\rangle + \gamma). \tag{1}$$

Because $E_v > E_e$, the transition $|e\rangle \to |g\rangle$ is second order in perturbation and the two steps cannot happen separately. In SM, RENP involves both electromagnetic and weak interactions. The E1-type photon emission $|v\rangle \to |g\rangle + \gamma$ is contributed by the electric dipole moment, while the M1-type neutrino pair emission $|e\rangle \to |v\rangle + \nu\bar{\nu}$ is mediated by the W/Z bosons. The weak Hamiltonian $\mathcal{H}_W \equiv \sqrt{2}G_F\left(v_{ij}J_V^\mu - a_{ij}J_A^\mu\right)\bar{\nu}_{iL}\gamma_\mu \nu_{jL}$ contains both the vector v_{ij} and the axial vector a_{ij} coefficients

$$a_{ij} \equiv U_{ei}U_{ej}^* - \frac{\delta_{ij}}{2}, \quad \text{and} \quad v_{ij} \equiv a_{ij} + 2\sin^2\theta_w \delta_{ij}, \tag{2}$$

where U_{ei} is the PMNS matrix element. The M1 transition selects only the axial part of $\mathcal{H}_W$.

The atomic spontaneous decay rate $\Gamma \sim G_F^2(E_e - E_g)^5/15\pi^3 \approx 10^{-34}\,\text{s}$ is extremely small [5]. Enhancing the decay is possible via two quantum mechanical effects [12]: stimulated photon emission and macroscopically coherent atoms [13]. The enhancing factors are proportional to the photon number density n_γ and the coherent atom number density n_a^2, respectively. The total decay width [14–16]

$$\Gamma \equiv \Gamma_0 \mathcal{I}(\omega), \quad \text{with} \quad \Gamma_0 \approx 0.002\,\text{s}^{-1}\frac{n_a^2 n_\gamma}{(10^{21}\,\text{cm}^{-3})^3}\left(\frac{V}{10^2\,\text{cm}^3}\right) \tag{3}$$

scales linearly with the material volume V. The spectral function $\mathcal{I}(\omega)$ is defined as

$$\mathcal{I}(\omega) \equiv \sum_{ij} \frac{\Delta_{ij}(\omega)}{(E_{vg} - \omega)^2}\Theta(\omega - \omega_{ij}^{\max})\left[|a_{ij}|^2 I_{ij}^{(D)} - \delta_M \text{Re}[a_{ij}^2]m_i m_j\right], \quad \text{with} \quad \omega_{ij}^{\max} \equiv \frac{E_e - E_g}{2} - \frac{1}{2}\frac{(m_i + m_j)^2}{(E_e - E_g)}, \tag{4}$$

where $q^2\Delta_{ij} \equiv \sqrt{[q^2 - (m_i + m_j)^2][q^2 - (m_i - m_j)^2]}$ with momentum transfer $q^2 \equiv (E_{eg}^2 - 2E_{eg}\omega)$ and $E_{ab} \equiv E_a - E_b$. The Heaviside Θ function imposes kinematics requirements on the frequency ω. Energy–momentum conservation allows the process to occur only if the trigger laser frequency ω is smaller than the a frequency threshold $\omega_{ij}^{\max}$ as a function of the emitted neutrino masses m_i and m_j.

The last term in the square bracket of Equation (4) is non-zero if neutrinos are Majorana particles ($\delta_M = 1$) and zero otherwise ($\delta_M = 0$). The first term appears in both cases, and is additionally a function of the neutrino masses

$$I_{ij}^{(D)} \equiv \frac{1}{3}\left\{E_{eg}(E_{eg} - 2\omega) - \frac{1}{2}(m_i^2 + m_j^2) + \frac{\omega^2}{2}\left[1 - \frac{1}{3}\Delta_{ij}(\omega)^2\right] - \frac{(E_{eg} - \omega)^2(\Delta m_{ij}^2)^2}{2E_{eg}^2(E_{eg} - 2\omega)^2}\right\}. \tag{5}$$

3. Non-Standard Interactions with Light Mediators

The W/Z gauge boson masses are much larger than the momentum transfer, and their propagators shrink to a contact term $1/(q^2 - m_{Z/W}^2) \approx 1/m_{Z/W}^2$. The relative size between the $m_{Z/W}^2$ scale and the atomic momentum transfer is $\sim 10^{21}$. For NSI with mediator mass of $1 \sim 100\,\text{keV}$, the decay width can be significantly enhanced over the SM one. In other words, RENP is very sensitive to light mediators.

3.1. Vector Mediators

The relevant new interactions with a vector-like mediator Z' are

$$\mathcal{L}_V = g^e \bar{e}\gamma^\mu \gamma_5 e Z'_\mu + \bar{\nu}_i \gamma^\mu (g_{L,ij}^\nu P_L + g_{R,ij}^\nu P_R)\nu_j Z'_\mu. \tag{6}$$

Because the neutrino pair emission transition ($|e\rangle \to |v\rangle$) is of the M1 type, it has even parity and selects the $\gamma_\mu\gamma_5$ component of the electron coupling. The neutrino interaction may contain both left and right axial currents, which generalizes Equation (2):

$$a_{ij}^L \equiv a_{ij} + \frac{g^e g_{L,ij}^\nu}{\sqrt{2}G_F(q^2 - m_{Z'}^2)}\delta_{ij}, \quad \text{and} \quad a_{ij}^R \equiv \frac{g^e g_{R,ij}^\nu}{\sqrt{2}G_F(q^2 - m_{Z'}^2)}\delta_{ij}. \tag{7}$$

The spectral function $\mathcal{I}(\omega)$ in Equation (4) becomes

$$\mathcal{I}_{Z'} \equiv \sum_{ij} \frac{\Delta_{ij}(\omega)\Theta(\omega - \omega_{ij}^{\max})}{(E_{vg} - \omega)^2} \left[\left(|a_{ij}^L|^2 + |a_{ij}^R|^2 - 2\delta_M \text{Re}[a_{ij}^L a_{ij}^R]\right)I_{ij}^{(D)} + \left(\delta_M \text{Re}\left[(a_{ij}^L)^2 + (a_{ij}^R)^2\right] - 2\text{Re}\left[a_{ij}^{L*}a_{ij}^R\right]\right)m_i m_j\right]. \tag{8}$$

In Figure 1, we present the $\mathcal{I}_{Z'}$ spectral function versus the trigger laser frequency ω. The lines have sudden dips around the kinematic thresholds. As expected, even for a tiny coupling $|g^e g_{L,ij}| \sim 10^{-16}$ (dashed red), the presence of a Z' mediator results in a sizable contribution when compared with the SM one (the black curve).
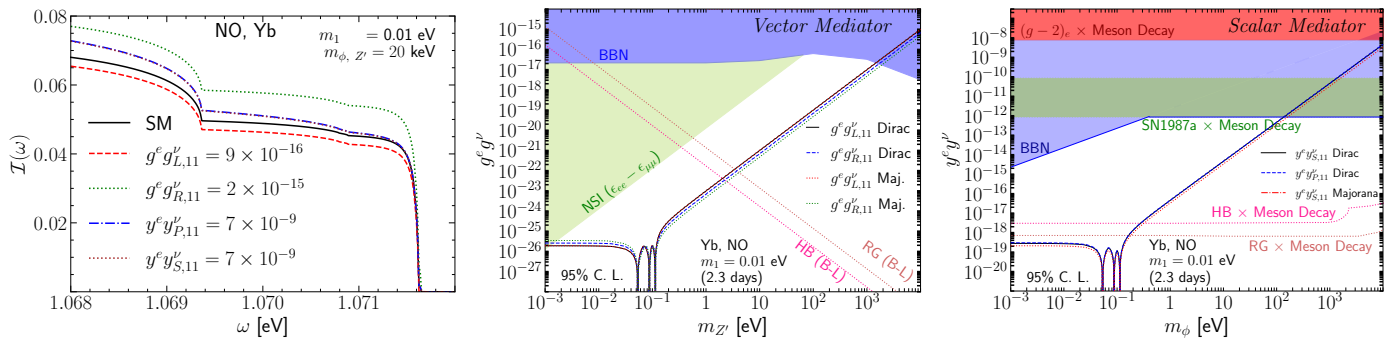

Figure 1. (**Left**) The spectral function $\mathcal{I}(\omega)$ of Yb as a function of the trigger laser frequency ω for the normal ordering and lightest neutrino mass $m_1 = 0.01$ eV for light vector/scalar mediators; also shown are the projected sensitivities for vector (**Middle**) and scalar (**Right**) mediators.

We estimate the sensitivity to the combination $|g^e g_{ij}^\nu|$ using the experimental setup proposed in [15]. The target is exposed to the trigger laser beam at three different frequencies $\omega_i = (1.0688, 1.0699, 1.0711)$ eV. The total number of events for each trigger laser frequency is obtained using the total decay width times exposure time T:

$$N(\omega) \equiv 0.002 \times \left(\frac{T}{s}\right) \frac{n_a^2 n_\gamma}{(10^{21} \text{ cm}^{-3})^3} \left(\frac{V}{100 \text{ cm}^3}\right) \mathcal{I}(\omega). \tag{9}$$

For $T = 2.3$ days, a target volume $V = 100$ cm^3, and $n_a = n_\gamma = 10^{21}$ cm^{-3}, we expect $\mathcal{O}(20)$ events at each ω_i. We use Poisson χ^2 [17] to compare the expected event numbers with and without new physics. The sensitivity curves are shown in the middle panel of Figure 1. Across almost the whole range from meV to keV, RENP can improve the sensitivity by 2~3 orders.

3.2. Scalar Mediator

A general spin-0 particle can couple with an electron via both scalar ($y_S^e \bar{e}e\phi$) and pseudo-scalar ($y_P^e \bar{e}\gamma_5 e\phi$) interactions. The M1 transition selects only the pseudo-scalar coupling to contribute. However, the neutrino side can have both types:

$$\mathcal{L}_\phi \equiv iy_P^e \bar{e}\gamma_5 e\phi + \bar{v}_i(y_{S,ij}^\nu + i\gamma_5 y_{P,ij}^\nu)v_j\phi + h.c. \tag{10}$$

Correspondingly, the spectral function becomes

$$\mathcal{I}_\phi = \sum_{ij} \frac{\Delta_{ij}(\omega)}{(E_{vg} - \omega)^2} \Theta(\omega - \omega_{ij}^{\text{max}}) \left[I_{ij}^{\text{SM}}(\omega) + \delta I_{ij}(\omega) \right], \tag{11}$$

where the correction term $\delta I_{ij}(\omega)$ is

$$
\begin{aligned}
\delta I_{ij} \quad \equiv \quad & \frac{|y^e|^2 \omega^2}{m_e^2 G_F^2} \frac{\left[|y_{S,ij}^\nu|^2 + (1 - \delta_M)|y_{P,ij}^\nu|^2 \right] E_{eg}(E_{eg} - 2\omega)}{24[E_{eg}(E_{eg} - 2\omega) - m_\phi^2]^2} - \frac{|y^e|^2 \omega^2}{m_e^2 G_F^2} \frac{|y_{S,ij}^\nu|^2 (m_i + m_j)^2 + (1 - \delta_M)|y_{P,ij}^\nu|^2 (m_i - m_j)^2}{24[E_{eg}(E_{eg} - 2\omega) - m_\phi^2]^2} \\
+ \quad & \frac{y^e \omega^2}{6\sqrt{2} G_F} \frac{\text{Re}\left[a_{ij} y_{S,ij}^\nu\right](m_i - m_j)\left[1 - \frac{(m_i + m_j)^2}{E_{eg}(E_{eg} - 2\omega)}\right]}{m_e[E_{eg}(E_{eg} - 2\omega) - m_\phi^2]} - (1 - \delta_M) \frac{\text{Im}\left[a_{ij} y_{P,ij}^\nu\right](m_i + m_j)\left[1 - \frac{(m_i - m_j)^2}{E_{eg}(E_{eg} - 2\omega)}\right]}{m_e[E_{eg}(E_{eg} - 2\omega) - m_\phi^2]}.
\end{aligned}
\tag{12}
$$

In addition, the left panel of Figure 1 shows the new contribution of the spectral function $\mathcal{I}_\phi$. Notice that the scalar coupling constant has to be larger than $|y^e y_{ij}^\nu| \sim 10^{-9}$ when compared with the vector one ($|g^e g_{L,ij}^\nu| \sim 10^{-15}$) to produce a similar change to the SM curve. This happens because nonrelativistic atomic transitions with pseudo-scalar couplings are suppressed by q^2/m_e^2, as $\langle e|\gamma_5|v\rangle \sim \mathbf{q} \cdot \langle e|\mathbf{S}|v\rangle/m_e$, where $\mathbf{S}$ is the spin operator. Consequently, the sensitivity to $|y^e y_{ij}^\nu|$ in the right panel of Figure 1 is five orders less stringent than the vector case, although it remains much better than the existing ones.

4. Neutrino Electromagnetic Moments

The neutrino magnetic (μ_ν) and electric (ϵ_ν) dipole moments are parameterized as [18]

$$H_M = \bar{\nu} \left[-(\mu_\nu)_{ij} i\sigma_{\mu\nu} q^\nu + (\epsilon_\nu)_{ij} \sigma_{\mu\nu} q^\nu \gamma_5 \right] \nu A^\mu(q). \tag{13}$$

A non-zero μ_ν (ϵ_ν) can be tested in various ways. The electron recoil measurements in neutrino and dark matter experiments provide a constraint $\mu_\nu^{\text{eff}} < 3 \times 10^{-11} \mu_B$ [19,20], where $\mu_B \equiv e/2m_e$ is the Bohr magneton. In addition, the red giant cooling due to plasmon decay ($\gamma^* \to \bar{\nu}\nu$) provides $\mu_\nu^\odot < 2.2 \times 10^{-12} \mu_B$ [21] and white dwarf pulsation/cooling puts $\mu_\nu^\odot < 2.9 \sim 7 \times 10^{-12} \mu_B$ [22–24] at 90% C.L. All these constraints have serious limitations. The astrophysical bounds are prone to various systematic uncertainties [25], while the electron recoil measurements only probe a combination of magnetic and electric moments with severe degeneracy and blind spots in the allowed parameter space [26].

In comparison, RENP does not suffer from any of these limitations. The decay rate for the magnetic (electric) moment, $\Gamma_M \equiv \Gamma_0 \sum_{ij} |(\mu_\nu)_{ij}|^2 \mathcal{I}_M^{ij}$ ($\Gamma_E \equiv \Gamma_0 \sum_{ij} |(\epsilon_\nu)_{ij}|^2 \mathcal{I}_E^{ij}$), with

$$\mathcal{I}_{\substack{M \\ E}}^{ij} \equiv \left(\frac{\mu_B}{G_F} \right)^2 \frac{\omega^2 \Delta_{ij} \Theta(\omega - \omega_{ij}^{\text{max}})}{9(E_{vg} - \omega)^2} \left[1 + \frac{(m_i \pm m_j)^2 \pm 4 m_i m_j}{q^2} - 2 \left(\frac{\Delta m_{ji}^2}{q^2} \right)^2 \right], \tag{14}$$

is a function of individual $(\mu_\nu)_{ij}$ or $(\epsilon_\nu)_{ij}$. These spectral functions are shown in the left and middle panels of Figure 2. The kinematic thresholds allow each non-zero contribution of $(\mu_\nu)_{ij}$ and $(\epsilon_\nu)_{ij}$ to be pinpointed, as well as for μ_ν to be separated from ϵ_ν. To accomplish this, instead of scanning three different frequencies, as in Section 3.1, we need to scan six: $\omega_i = (1.069, 1.07, 1.0708, 1.0712, 1.0716, 1.07164)$ eV. In this way, along with the individual matrix element, we can identify another one, $\omega = 1.068$ eV, to disentangle μ_ν from ϵ_ν. The sensitivity in the right panel of Figure 2 as a function of the exposure time is competitive with current experiments, and can be further improved with longer exposure time.
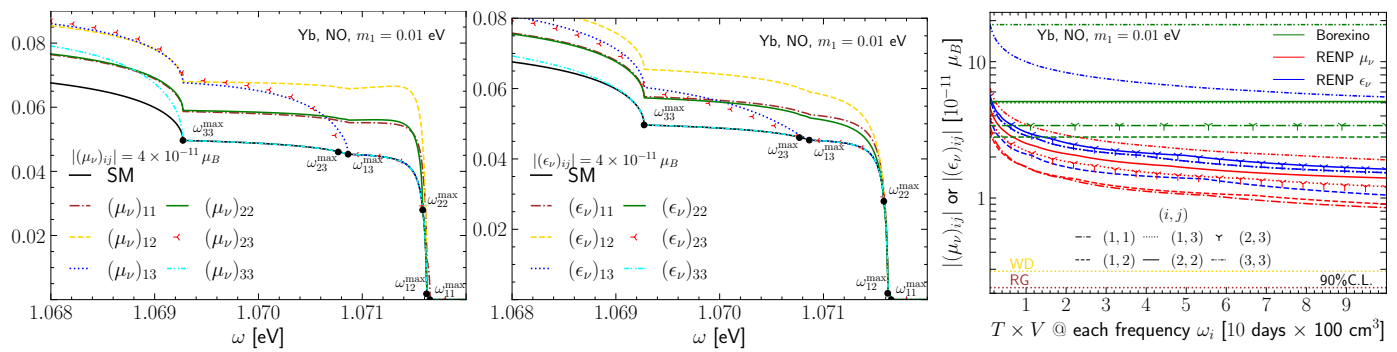
Figure 2. The first two panels show the spectral functions for the electric (**Left**) and magnetic (**Middle**) moments; also shown are the projected sensitivities for various elements of the neutrino electromagnetic moments (**Right**). In all cases, we use normal ordering and take the lightest neutrino mass to be $m_1 = 0.01$ eV.

5. Conclusions

We have presented the novel idea of using the atomic radiative emission of neutrino pairs to probe the neutrino NSI with light mediators. The typical $\mathcal{O}(\mathrm{eV})$ atomic transition energy improves current constants by several orders of magnitude for vector and scalar mediators with masses below keV. With the photon being a massless mediator, the searching neutrino magnetic moments additionally benefits from the eV momentum transfer of RENP. Most importantly, the kinematics thresholds allow different coupling constants to be separated and their individual matrix elements to be identified, which is not possible for current probes.

6. Notes Added

Constraints on light mediators and neutrino electromagnetic properties exist from various sources. A detailed survey of the current bounds can be found in our third paper on RENP [27], which appears after the submission of this proceeding. The two most recent constraints are due to the DM detection, $|\mu^{\odot}| \equiv |\widetilde{U}_{ej}|^2 |(\mu_\nu)_{ij} - i(\epsilon_\nu)_{ij}|^2 < 6 \times 10^{-12}\,\mu_B$ [28], and coherent nuclei scatterings experiments, $|\mu^{\mathrm{eff}}_\alpha|^2 \equiv \sum_{ij}\left\{ U_{\alpha i}(\mu_\nu^2 + \epsilon_\nu^2)_{ij}U^*_{\alpha j} + 2\,\mathrm{Im}[U_{\alpha i}(\mu_\nu \epsilon_\nu)_{ij}U^*_{\alpha j}] \right\}$, with the current bounds being $|\mu^{\mathrm{eff}}_e|^2 < 4 \times 10^{-9}\,\mu_B$ and $|\mu^{\mathrm{eff}}_\mu|^2 < 4 \times 10^{-10}\,\mu_B$ [29]. While the RENP experiment can achieve similar bounds to coherent scattering within a few days, it should take more than a hundred days to obtain bounds comparable to the DM direct detection measurements. However, the neutrino mass eigenstates cannot be disentangled in either DM or coherent scattering experiments. Consequently, the bounds always involve a combination of the neutrino mixing matrix elements. In contrast, the RENP process does not suffer from such degeneracies. The detection of the kinematics thresholds together with scanning of the photon frequency spectrum allows for the separation of the individual matrix elements of each interaction type. In this sense, the RENP experiment is a unique probe of neutrino interactions and light mediators.

Data Availability Statement: All the codes used in this work can be shared uppon request.

Conflicts of Interest: The authors declare no conflicts of interest.

References

1. Farzan, Y.; Tortola, M. Neutrino oscillations and Non-Standard Interactions. *Front. Phys.* **2018**, *6*, 10. [CrossRef]
2. Bhupal Dev, P.S.; Babu, K.S.; Denton, P.B.; Machado, P.A.N.; Argüelles, C.A.; Barrow, J.L.; Chatterjee, S.S.; Chen, M.C.; de Gouvêa, A.; Dutta, B.; et al. Neutrino Non-Standard Interactions: A Status Report. *SciPost Phys. Proc.* **2019**, *2*, 001. [CrossRef]
3. Smirnov, A.Y.; Xu, X.J. Wolfenstein potentials for neutrinos induced by ultra-light mediators. *J. High Energy Phys.* **2019**, *12*, 046. [CrossRef]
4. Babu, K.S.; Chauhan, G.; Bhupal Dev, P.S. Neutrino nonstandard interactions via light scalars in the Earth, Sun, supernovae, and the early Universe. *Phys. Rev. D* **2020**, *101*, 095029. [CrossRef]
5. Yoshimura, M. Neutrino Pair Emission from Excited Atoms. *Phys. Rev. D* **2007**, *75*, 113007. [CrossRef]
6. Fukumi, A.; Kuma, S.; Miyamoto, Y.; Nakajima, K.; Nakano, I.; Nanjo, H.; Ohae, C.; Sasao, N.; Tanaka, M.; Taniguchi, T.; et al. Neutrino Spectroscopy with Atoms and Molecules. *Prog. Theor. Exp. Phys.* **2012**, *2012*, 04D002. [CrossRef]
7. Hiraki, T.; Hara, H.; Miyamoto, Y.; Imamura, K.; Masuda, T.; Sasao, N.; Uetake, S.; Yoshimi, A.; Yoshimura, K.; Yoshimura, M. Coherent two-photon emission from hydrogen molecules excited by counter-propagating laser pulses. *J. Phys. B* **2019**, *52*, 045401. [CrossRef]
8. Tashiro, M.; Das, B.P.; Ekman, J.; Jönsson, P.; Sasao, N.; Yoshimura, M. Macro-coherent radiative emission of neutrino pair between parity-even atomic states. *Eur. Phys. J. C* **2019**, *79*, 907. [CrossRef]
9. Ge, S.F.; Pasquini, P. Probing light mediators in the radiative emission of neutrino pair. *Eur. Phys. J. C* **2022**, *82*, 208. [CrossRef]
10. Ge, S.F.; Pasquini, P. Unique Probe of Neutrino Electromagnetic Moments with Radiative Pair Emission. *Phys. Lett. B* **2023**, *841*, 137911. [CrossRef]
11. Yoshimura, M. Solitons and Precision Neutrino Mass Spectroscopy. *Phys. Lett. B* **2011**, *699*, 123–128. [CrossRef]
12. Yoshimura, M.; Sasao, N.; Tanaka, M. Dynamics of paired superradiance. *Phys. Rev. A* **2012**, *86*, 013812. [CrossRef]
13. Dicke, R.H. Coherence in Spontaneous Radiation Processes. *Phys. Rev.* **1954**, *93*, 99–110. [CrossRef]
14. Dinh, D.N.; Petcov, S.T.; Sasao, N.; Tanaka, M.; Yoshimura, M. Observables in Neutrino Mass Spectroscopy Using Atoms. *Phys. Lett. B* **2013**, *719*, 154–163. [CrossRef]
15. Song, N.; Garcia, R.B.; Gomez-Cadenas, J.J.; Gonzalez-Garcia, M.C.; Conde, A.P.; Taron, J. Conditions for Statistical Determination of the Neutrino Mass Spectrum in Radiative Emission of Neutrino Pairs in Atoms. *Phys. Rev. D* **2016**, *93*, 013020. [CrossRef]
16. Zhang, J.; Zhou, S. Improved Statistical Determination of Absolute Neutrino Masses via Radiative Emission of Neutrino Pairs from Atoms. *Phys. Rev. D* **2016**, *93*, 113020. [CrossRef]
17. Particle Data Group; Zyla, P.A.; Barnett, R.M.; Beringer, J.; Dahl, O.; Dwyer, D.A.; Groom, D.E.; Lin, C.-J.; Lugovsky, K.S.; Pianori, E.; et al. Review of Particle Physics. *Prog. Theor. Exp. Phys.* **2020**, *2020*, 083C01. [CrossRef]
18. Giunti, C.; Studenikin, A. Neutrino electromagnetic interactions: A window to new physics. *Rev. Mod. Phys.* **2015**, *87*, 531. [CrossRef]
19. Beda, A.G.; Brudanin, V.B.; Egorov, V.G.; Medvedev, D.V.; Pogosov, V.S.; Shevchik, E.A.; Shirchenko, M.V.; Starostin, A.S.; Zhitnikov, I.V. Gemma experiment: The results of neutrino magnetic moment search. *Phys. Part. Nucl. Lett.* **2013**, *10*, 139–143. [CrossRef]
20. Agostini, M.; Altenmüller, K.; Appel, S.; Atroshchenko, V.; Bagdasarian, Z.; Basilico, D.; Bellini, G.; Benziger, J.; Bick, D.; Bonfini, G.; et al. Limiting neutrino magnetic moments with Borexino Phase-II solar neutrino data. *Phys. Rev. D* **2017**, *96*, 091103. [CrossRef]
21. Díaz, S.A.; Schröder, K.P.; Zuber, K.; Jack, D.; Barrios, E.E.B. Constraint on the axion-electron coupling constant and the neutrino magnetic dipole moment by using the tip-RGB luminosity of fifty globular clusters. *arXiv* **2019**, arXiv:1910.10568.
22. Córsico, A.H.; Althaus, L.G.; Bertolami, M.M.M.; Kepler, S.O.; García-Berro, E. Constraining the neutrino magnetic dipole moment from white dwarf pulsations. *J. Cosmol. Astropart. Phys.* **2014**, *8*, 054. [CrossRef]
23. Bertolami, M.M.M. Limits on the neutrino magnetic dipole moment from the luminosity function of hot white dwarfs. *Astron. Astrophys.* **2014**, *562*, A123. [CrossRef]
24. Hansen, B.M.S.; Richer, H.; Kalirai, J.; Goldsbury, R.; Frewen, S.; Heyl, J. Constraining Neutrino Cooling using the Hot White Dwarf Luminosity Function in the Globular Cluster 47 Tucanae. *Astrophys. J.* **2015**, *809*, 141. [CrossRef]
25. Stancliffe, R.J.; Fossati, L.; Passy, J.-C.; Schneider, F.R.N. Confronting uncertainties in stellar physics. II. Exploring differences in main-sequence stellar evolution tracks. *Astron. Astrophys.* **2016**, *586*, A119. [CrossRef]
26. Sierra, D.A.; Miranda, O.G.; Papoulias, D.K.; Garcia, G.S. Neutrino magnetic and electric dipole moments: From measurements to parameter space. *Phys. Rev. D* **2022**, *105*, 035027. [CrossRef]
27. Ge, S.F.; Pasquini, P. Disentangle Neutrino Electromagnetic Properties with Atomic Radiative Pair Emission. *arXiv* **2023**, arXiv:2306.12953.

28. Khan, A.N. Light new physics and neutrino electromagnetic interactions in XENONnT. *Phys. Lett. B* **2023**, *837*, 137650. [CrossRef]
29. Khan, A.N. Neutrino millicharge and other electromagnetic interactions with COHERENT-2021 data. *Nucl. Phys. B* **2023**, *986*, 116064. [CrossRef]